ICANS XIX,
19th meeting on Collaboration of Advanced Neutron Sources
March 8 – 12, 2010
Grindelwald, Switzerland

DESIGN STUDY OF A SPECTROSCOPIC IMAGING LINE AT J-PARC MLF

Y. Kiyanagi, T. Kamiyama, H. Satoh
Graduate School of Engineering, Hokkaido University
Kita-13, Nishi-8, Kita-ku, Sapporo, 060-8628, Japan

and

T. Shinohara, S. Takada, K. Aizaw, M. Arai,
T. Kai, M. Harada, K. Sakai, K. Oikawa, M. Ooi, and F. Maekawa,
J-PARC Center, JAEA

H. Hayashida, T. Sakai, and M. Matsubayashi
Quantum Beam Science Directorate, JAEA

M. Segawa, and M. Kureta
Nuclear Science and Engineering Directorate, JAEA
2-4 Shirakata-shirane, Tokai-mura, Naka-gun, Ibaraki-ken, 319-1195, Japan

ABSTRACT

We are considering an imaging beam line at MLF (Materials and Life science experimental Facility) at J-PARC. In the pulsed neutron imaging we use the resonance absorption and the Bragg edge scattering as well as the traditional low energy neutron interaction. There are three types of moderators: coupled, decoupled and poisoned. In the resonance energy region, the neutronic characteristics are almost the same among them. For the Bragg edge analysis it is desired to attain a high time resolution around 0.1%, but the value is almost impossible with reasonable length and intensity at the coupled moderator. We can attain the high time resolution at the poisoned moderator. On the other hand, other applications such as polarized neutron imaging for magnetic fields do not require such high time resolution. Therefore, as a result it is concluded that a beam line at the decoupled moderator will be the best compromise for all applications.

1. Introduction

Energy selective neutron imaging is expected to open the new field of the neutron radio graphy. At the stedy state neutron sources this type of imaging give different contrast imaging depending on the total neutron cross section at the selective energy, which may give more information on an objective. At the pulsed neutron source we can use the time-of-flight method for energy analysis. A 2-dimensional position-sensitive detector combined with the pulsed neutron source give imaging data as a function of neutron flight time. By analyzing this kind of data we can get information of the object on texture and/or crystal structure of the material, elements in the object, and so on [1-4]. The pulsed neutron imaging is still under development. However, it has possibility to give much informative data than the traditional steady state neutron imaging.

In Japan a high intensity pulsed neutron source, JSNS (Japan Spallation Neutron Source) at J-PARC MLF (Material Life science experimental Facility) is under operation. We are performing the pulsed neutron imaging at the beam line 10 (BL10), NOBORU and intending to construct a beam line at MLF.

For the design of the imaging beam line not only the L/D but also the wavelength resolution is important. Therefore, first we have to choose a moderator among three moderators at JSNS under the consideration of various methods performed at the pulsed neutron source. Here, we present our consideration on the design of the imaging beam line at J-PARC MLF.

2. Required characteristics for pulsed neutron imaging beam line

Here, we consider three types of measurements for the imaging in order to consider the best moderator and the suitable flight path lengths at J-PARC MLF

2.1. Bragg Edge Imaging

Bragg edge transmission (BET) spectra shown in Fig. 2.1.1, obtained by a neutron imaging detector coupled with a time-of-flight (TOF) spectroscopy at a pulsed source, can simultaneously and quantitatively give spatial distributions of crystal structure [1], crystalline phase [1], texture [2,3], microstructure [3] and strain [4] in a polycrystalline material. Such crystallographic images are very useful for materials design. For quantitative imaging of crystallographic information with high precision, 2D real-space BET spectra should be analyzed by individual edge profile analysis method, in a simillar way of Pawley analysis method and Rietveld analysis method such as TOF powder diffractometry. For this reason, a pulsed neutron spectroscopic BET imaging instrument should be designed under the same concepts as a diffractometer.

The prior requirements are (1) enough resolution of lattice spacing (*d*-spacing) $\Delta d/d$ for crystal structure and strain refinements, (2) wider wavelength band width for measurements of longer *d*-spacing materials, (3) higher flux for in-situ and precise measurements and (4) better beam collimation ratio L/D for radiography. First of all, we aimed at $\Delta d/d$ = 0.15 % ~ 0.20 % for strain imaging. This value came from the resolution values of BL19 (the strain/stress analysis diffractometer TAKUMI [5]) and BL20 (the versatile powder diffractometer iMATERIA [6]) in J-PARC. In a Bragg edge transmission, $\Delta d/d$ can be directly given by $\Delta t/t$, where Δt is the FWHM (Full Width of Half Maximum) of a neutron pulse emitted from the moderator and t is the neutron flight time from the moderator to the detector. This principle is owing to direct observation of backscattered neutrons in a transmission geometry, derived from that a Bragg edge of crystal-lattice-planes $\{hkl\}$ can appear only at $\lambda = 2d_{hkl} \sin 90°$. Figure 2.1.2 shows the calculation results of the worst $\Delta d/d$ line as a function of neutron flight distance in low-energy neutrons (in fact, at λ = 0.4 nm), estimated from the simulation data [7] about 4 type moderators; the coupled moderator (called CM, for the highest intensity), the decoupled moderator (DM, for meadium resolution), the thicker poisoned-decoupled moderator (PM+, for higher resolution) and the thinner poisoned-decoupled moderator (PM-, for the highest resolution). The beam line viewing PM- or PM+ can easily achieve the required resolution at the flight path length from 10 m to 20 m. In case of a CM beam-line, we need more than 68 m flight path length.

Table 2.1.1 shows the summary of various performances of each beam-line instaled at a CM, DM, PM+ or PM-, without supermirror guides. Here, we considered the $\Delta d/d$ = 0.20 % case and the $\Delta d/d$ = 0.15 % case. They were estimated from the simulation data [7] and the experimental data [1,2,8] measured at BL10 (the test port NOBORU [9]) viewing DM. The PM-, PM+ and DM based beam-lines can give a relatively wide wavelength band width owing to sharp neutron pulses. The CM based long beam-line can give the highest collimation ratio, but sufferes from low flux because a lot of neutrons are dumped by a frame overlap chopper. In case of the same $\Delta d/d$ (high resolution; 0.15 % ~ 0.20 %), the PM+ based beam-line is the best due to highest intesity, so the measurement time is 1 ~ 60 minutes for Fe or Mg alloys, and also to the widest wavelength band (~ 0.77 nm or more). For this measurement time, it is necessary to develop the detectors with the spatial resolutin of less than 1 mm and the counting rate of more than 10 MHz.

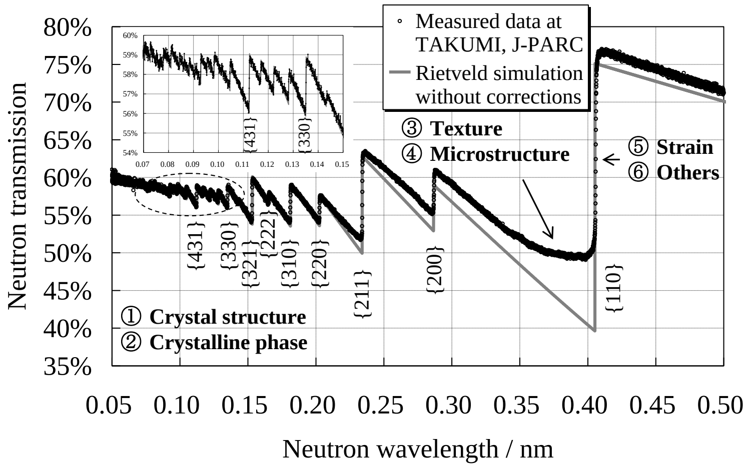

Figure 2.1.1: Bragg edge transmission spectrum of a rolled α-Fe plate of 5 mm thickness, and crystallographic information obtained by its spectral analysis. We measured this high *d*-spacing resolution spectrum in TAKUMI [5] spectrometer located at 40 m from the thicker poisoned-decoupled moderator (PM+) in J-PARC, by using the 16×16 pixel type ^{6}Li-glass scintillation imaging detector [8].

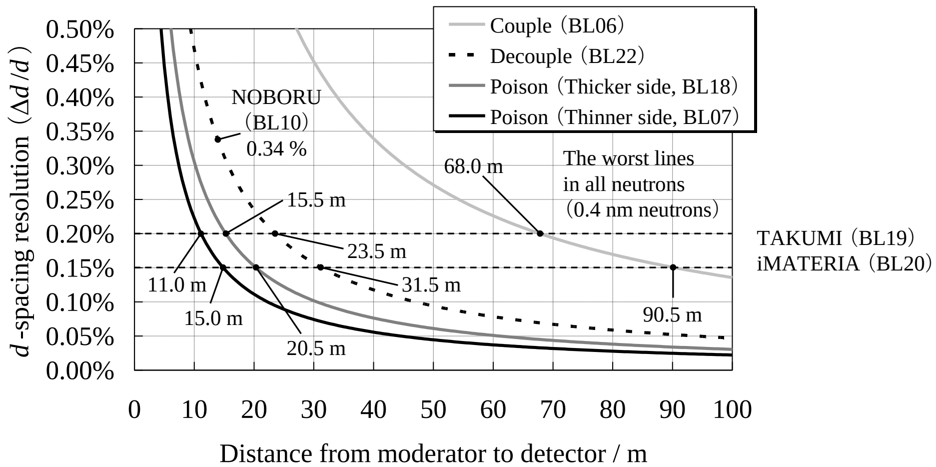

Figure 2.1.2: Beam-line and detector position dependency of the resolution $\Delta d/d$. Required resolutions, $\Delta d/d$ of 0.20 % or 0.15 %, are attained at 11.0 m / 15.0 m (PM-), 15.5 m / 20.5 m (PM+), 23.5 m / 31.5 m (DM) and 68.0 m / 90.5 m (CM), respectively.

Table 2.1.1: Summary of instrumental parameters of each beam-line of the 0.20 % or 0.15 % resolution, without supermirrors. In this table, ① ~ ④ represent the ranking of the important parameters between the beam-lines. For a spectroscopic BET imaging at J-PARC, the utilization of PM or DM is recommended because of the higher *d*-spacing resolution, the wider wavelength band width and the shorter measurement time. However, the high efficiency and counting rate detector will be required for the full performances.

Choice of moderator and flight path length for achieving $\Delta d/d$ of 0.20 % or 0.15 %	**CM (BL06)** 68.0 m / 90.5 m	**DM (BL22)** 23.5 m / 31.5 m	**PM+ (BL18)** 15.5 m / 20.5 m	**PM- (BL07)** 11.0 m / 15.0 m
Available wavelength band limit @ 25 Hz / nm	0.23 / 0.17 ④	0.67 / 0.50 ③	1.02 / 0.77 ②	1.44 / 1.05 ①
Time-averaged cold neutron flux† / $cm^{-2}s^{-1}$	6.4×10^{6} †† / 2.5×10^{6} †††	1.6×10^{7} / 7.7×10^{6}	1.8×10^{7} / 9.9×10^{6}	1.7×10^{7} / 8.8×10^{6}
Pulse FWHM Δt @ 0.4 nm / μs	138.5	48.0	31.2	22.7
Evaluation of neutron pulse tail	④	③	②	①
FOM (Intensity / $FWHM^2$) ratio @ 0.4 nm	1.0	3.6	5.9	6.5
Beam collimation ratio L/D without pinholes	680 / 905 ①	235 / 315 ②	155 / 205 ③	110 / 150 ④
Measurement time of strain imaging / min for 1 mm^2/pixel & $\Delta t\times0.05$ μs TOF-analysis in case of 10000 counts for 0.4 nm neutrons	54.0†† / 191.1††† ④	25.7 / 61.9 ②	24.4 / 56.3 ①	26.3 / 66.5 ③
Measurement time of the others imaging / min for 1 mm^2/pixel & $\Delta t\times0.5$ μs TOF-analysis in case of 5000 counts for 0.4 nm neutrons	2.7†† / 9.6†††	1.3 / 3.1	1.2 / 2.8	1.3 / 3.3
Maximum instantaneous counting rate / MHz/mm^2	1.95 / 0.83 ①	5.91 / 2.45 ②	9.60 / 4.15 ③	12.25 / 4.83 ④
Total evaluation for spectroscopic BET imaging	×	○	◎	△

† Considering to use a 25 Hz frame-overlap-chopper
†† Considering to use a 25/2 Hz frame-overlap-chopper for using 0.4 nm neutrons
††† Considering to use a 25/3 Hz frame-overlap-chopper for using 0.4 nm neutrons

2.2. Polarized Neutron Imaging

Visualization of the magnetic field is one of the most exciting applications for the neutron imaging technique and suite to the pulsed neutron source due to the time of flight measurement. For example, this technique can be used to study the spatial magnetic field distribution inside the closed space or to visualize the magnetic domain structure of magnetic materials. The neutron spin motion at a passage through a magnetic field is described by a simple equation, $\frac{\mathrm{d}}{\mathrm{d}t}\boldsymbol{\sigma}(t) = \gamma\boldsymbol{\sigma}(t) \times \boldsymbol{B}(t)$, where $\boldsymbol{\sigma}(t)$ is the unit vector parallel to the neutron spin, γ is gyromagnetic ratio of the neutron and $\boldsymbol{B}(t)$ is a external magnetic field. Accordingly, the neutron spin experiences a Larmor precession in a magnetic field with a frequency ω_L proportional to the magnetic field strength, thus the precession angle φ can be written by the product of precession frequency ω_L and the flight time in the field. In other words, this angle φ depends on the path integral of magnetic field in which neutron transverse and the neutron wavelength λ. Thus, the monochromatized neutron beam is indispensable for the magnetic field imaging. In this sense, the usage of pulsed neutrons, which are intrinsically monochromatic at each instant, gives us an opportunity to treat the strength of magnetic field quantitatively, by studying the wavelength dependence of the transmitted neutron polarization using the TOF method with high efficiency. Moreover, we can obtain the information about the direction of magnetic field by the selection of the analyzing direction neutron spins.

The requirements for the pulsed neutron beam line to perform the magnetic field imaging experiment using polarized neutrons are considered as follows. At first, the usability of a broad wavelength band width is necessary for the magnetic field imaging, because analyzing the neutron polarization in broad wavelength range makes it possible to determine the magnetic field strength very precisely. In the point of magnetic field sensitivity, a longer wavelength neutron has an advantage to observe a small magnetic field as it stays for a long time in the field, on the contrary, a shorter wavelength neutron is important to observe large one. Thus, the distance between neutron source and the detector should be short. Then, the resolution of neutron spin rotation angle mainly depends on the wavelength resolution, and a good resolution is required for a large magnetic field observation. Therefore, a pulsed neutron beam with a sharp pulse width is preferable for this imaging technique. Next, installation of good neutron optical devices for the neutron polarization and the polarization analysis and importing new techniques on polarized neutron into the imaging experiments should be installed. Required specifications for the polarizer/analyzer are as follows, a large aperture, high polarizability with high transmission, wide available wavelength range especially toward shorter wavelength region. To determine the magnetic field direction, application of the neutron polarimetry technique to the magnetic field imaging is essential, and the use of spin phase or neutron spin interference earns high sensitivity for smaller magnetic field. Moreover, combination of the tomography will bring about the chance to reconstruct 3D magnetic field distribution.

2.3. Reonance Imaging

Neutron resonance absorption spectroscopy (N-RAS) can measure the dynamics of atoms by analyzing the Doppler broadening of their resonance spectra. The method enables us to investigate motions of a particular element, because the resonance energies are peculiar to the element [10]. Then, N-RAS can be applied to the microchemical analysis or dynamical analysis of the small amount components [11]. Especially, with usage of a 2-dimensional neutron detector and TOF technique we can obtain the distribution of the neutron resonance absorption spectra on the corresponding sample plane [12].

For carrying such N-RAS imaging we have to consider about some factors such as the applied energy region, the energy resolution or the neutron pulse shape. The energy region which we need for the N-RAS measurement is at least 1 to 1000 eV for the aim of the chemical element analysis, for example S has the minimum energy resonance peak at 200 eV and Cl at 400 eV. For the atomic dynamics characterization with N-RAS we need the flight time resolution $\Delta t/t$ ~ 1 % that can lead the temperature difference ΔT ~ 10 K in our analysis about Ta 4.28 eV peak. Under such preconditions we have calculated instrumental parameters on the base of J-PARC MLF moderator simulations [7].

Figure 2.3.1 shows the examples of calculated $\Delta t/t$ versus neutron flight length for the monochromatic neutron energy. From the figure $\Delta t/t$ ~ 1 % is achieved over 7 m of flight length at both energies for all moderator types. This dependency is the same up to 1000 eV. Less than 40 eV the DM moderator has the highest resolution and at higher energy region the resolution change among moderators disappears. Then the DM is better from the $\Delta t/t$ point of view. The peak intensities for respective moderators versus energy are shown in Fig. 2.3.2. As shown in the figure the intensities are almost coinciding, but PM- has just a small fault in intensity.

The energy dependence of the pulse shapes are shown in Fig. 2.3.3. At low energy region less than 100 eV DM has a fine shape with the higher peak. CM has a broader peak width and a long tail, and the PM+ and PM- have slightly collapsed shapes. On the higher energy their shapes become resemble form, but the CM has a broader half width than others. The pulse shape is very important for the peak shape analysis of the resonance peak which leads the characterization of atomic dynamics. The DM is the best choice from the neutron pulse shape.

For the chemical analysis the peak separation ability in high energy region is important. Especially, because one MLF neutron pulse is made from two J-PARC proton bunches, that affects the resonance peak shape. We performed the resonance spectrum measurement on the beam line at MLF. The peak split by the proton bunch was recognized. We estimate the peak split ability based on the spectrum. The 115 eV peak can be confirmed splitting. The spectrum was obtained under the conditions of the flight length 29 m, the time channel width 40 ns and the proton bunch split 599 ns. The rough estimate of the splitting energy from here is twice of the full width of half maximum of the neutron pulse. This resolution $\delta e/E$ is shown in figure 2.3.5. When we use the DM, $\delta e/E$ becomes < 1.8 % at the flight length 15 m, < 1 % at 27 m.

As conclusion the DM beam line at the J-PARC MLF is the best for the N-RAS imaging. The time resolution, the neutron intensity and the peak shape are desirable for the usage of epithermal neutron over flight length 15 m. From the peak splitting ability the selectable flight length is better to the any kind of experiments, intensity or resolution important.

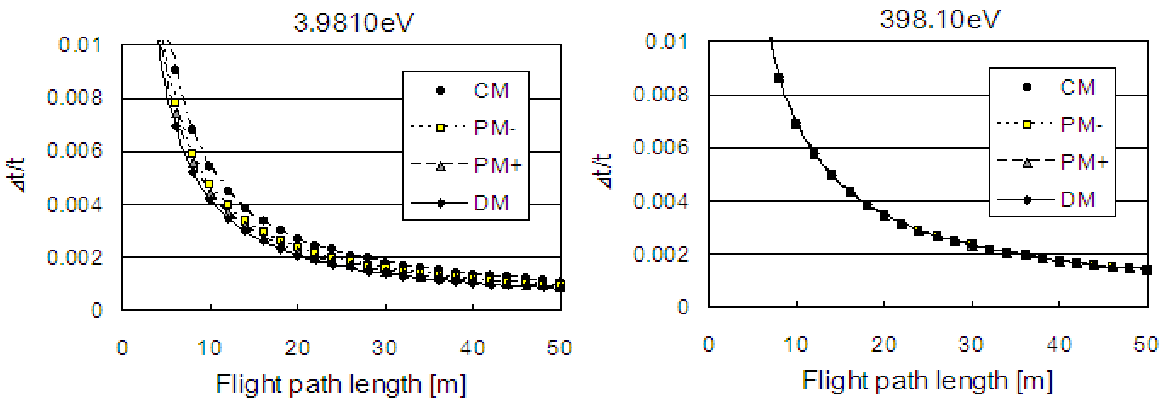

Fig. 2.3.1. The flight time resolution $\Delta t/t$ at neutron energy 3.9810 eV and 398.10 eV.

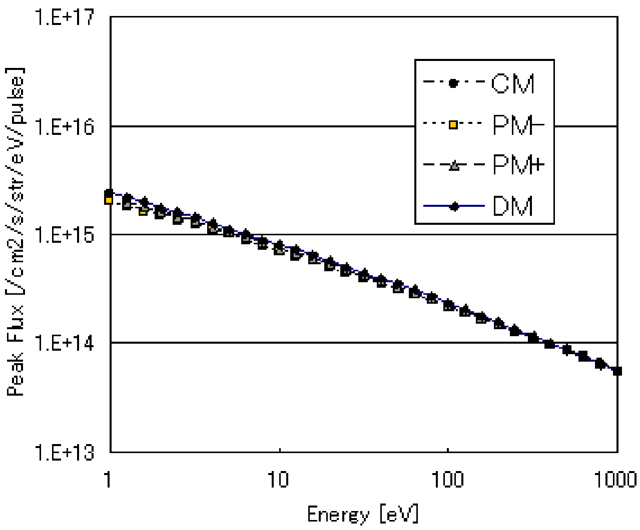

Fig. 2.3.2. The calculated peak intensities for each moderator type of J-PARC MLF.

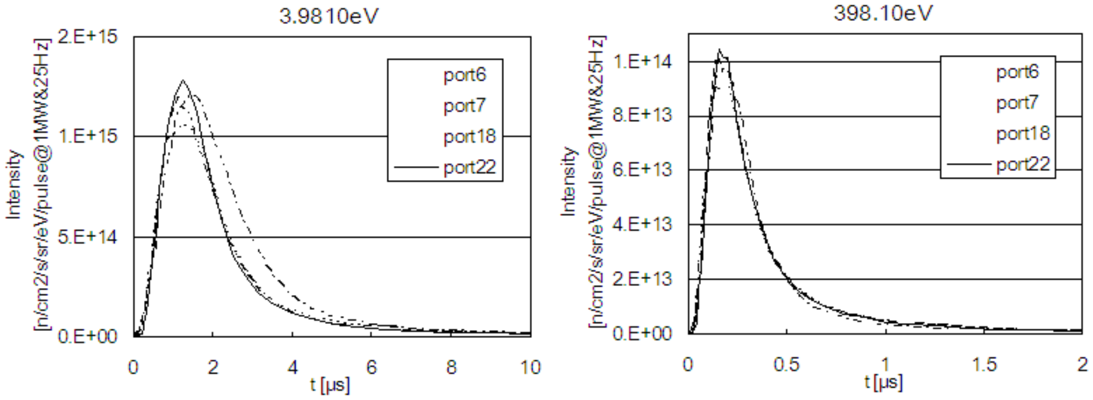

Fig. 2.3.3. The simulated peak shape at neutron energy 3.981 eV and 398.10 eV.

3. Beam Line Design

From the discussions in the previous section, only the strain measurement need the poisoned moderator and other's requirements match the performance of the decoupled moderator. The experiment obtaining the texture information by the analysis of the Bragg peaks also does not need the high wavelength resolution, although this type of experiment was not discussed. The starain analysis is possible at DM beamline at a position of more than 20m. Therefore, we decided to use the DM for the J-PARC imaging beam line.

To meet required characteristics for this instrument, high flexibility is indispensable for the beam line design. Here, we present the basic idea of the beam line components and experimental cave as follows. Figure 3.1 is a very preliminary but ideal drawing for the J-PARC beam line at present, and this structure is changed after the decision of the beam line number for the imaging.

i) Shutter insert and bulkshield insert
Ni coated natural neutron guide or low-Qc supermirror one with cross-section of 100 mm x 100 mm (= size of the moderator viewed surface) would be installed in 2.3 - 7.3 m section to increase the divergence of low-energy neutrons. This will be used only for high intensity measurements.

ii) Rotary collimator
Beam divergence can be changed by use of a rotary collimator (RC) that will be installed at uppermost stream of experimental hall, which will make pinhole at 7.7 m from the moderator as shown in Fig. 3.1. The RC would have four holes; one is fully opened (i.e. 100 mm x 100 mm) and the others have different pinhole size. The pinhole will be made by steel and polyethylene. Its effectiveness is already confirmed at NOBORU (BL10 of MLF).

iii) Bandwidth choppers and T0 chopper
Bandwidth chopper (BWC) will be installed to eliminate so called frame overlap neutrons. Because the total flight path length changes considerably in this instrument, bandwidth have to be matched by phasing two counter rotated BWCs.

T0 chopper, which suppresses high-energy neutrons and flashed gamma-ray mainly came from the moderator, will be installed just after the BWCs. This chopper will be operated when thermal and/or cold neutron will be mainly used, whereas it will be stopped at opening position for resonance neutron imaging experiment.

iv) Exchangeable optics
Exchangeable neutron optics parts will be equipped following the choppers. The components such as filters (Bi, Cd, etc…), polarizer with spin flipper, neutron lens system, Sollar slits and narrowers are now under consideration. These items have to be switched as required.

v) Experimental area
If the pinhole will be made at 7.7 m position in the rotary collimator, the beam size of 200 mm x 200 mm can be realized at L1 = 23.1 m. We note this position as 'Rearmost Position' in Fig. 3.1. Here, L/D value about 5000 can be achieved by use of 3 mm pinhole at 7.7 m.

'Forefront Position' will be used for the high-intensity measurement such as real-time tomography. Low-energy neutrons down to 1 meV also easy to use at this position.

A sample stage consist of goniometer should have sufficient load capacity, for example, 1 ton. Circles of diameter 1200 mm are shown in Fig. 3.1 for guide to the eye. The stage can be moved between forefront and rearmost positions along the floor guide rail. This feature may be very useful for the contrast imaging technique. Adjustable vacuum pipe are required to minimize air scatter.

Floor space in the cave would be adequate as shown in Fig. 3.1, however, the height of 3.8 m might be minimum.

Because of the large volume sample could be highly radioactive, temporal sample storage area should be allocated inside the experimental cave, which is also shown in Fig. 3.1.

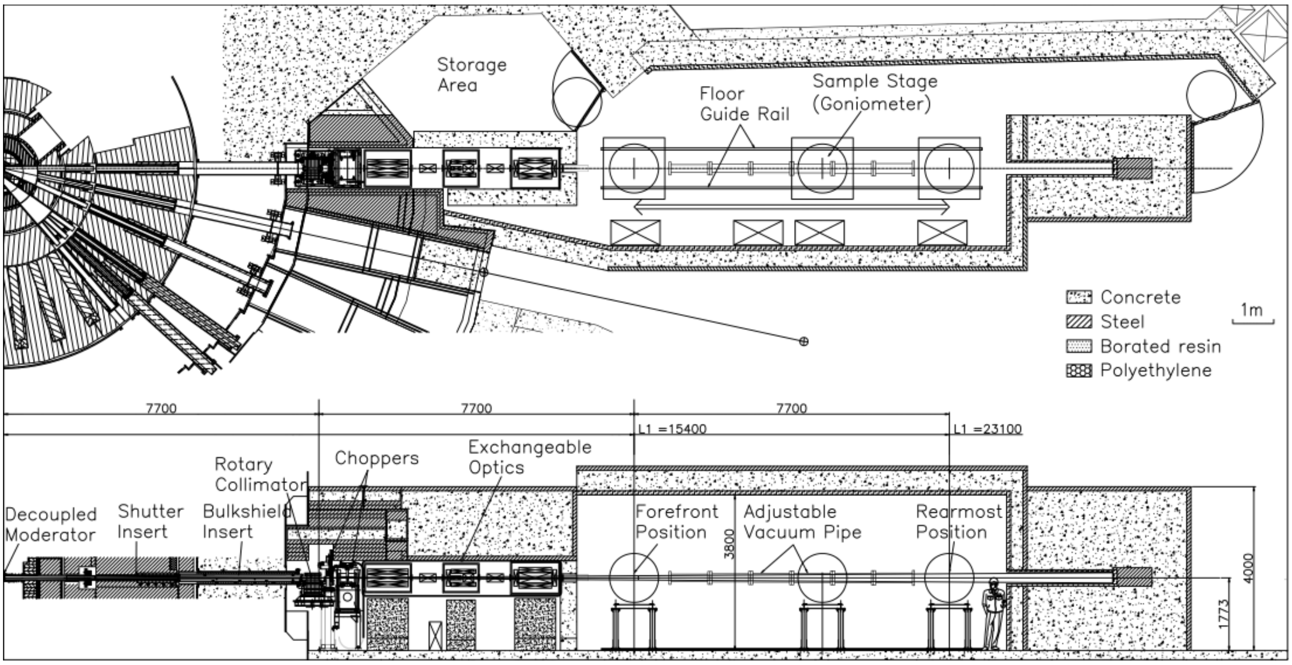

Fig. 3.1 Very pleliminary beam line sketch of the imaging instrument.

4. Conclusion

We have considered the design items for the imaging beam line at J-PARC MLF. Requirements of many applications matched the DM performance. Therefore, we decided to use the beam line viewing the DM and made a very preliminary sketch of the imaging beam line. However, in future we need the discussion on the choice of the beam line at J-PARC MLF, and after then detailed design should be performed. We are intending to make proposal to J-PARC in the near future.

5. References

1. Y. Kiyanagi, H. Sato, O. Takada, N. Ayukawa and T. Kamiyama, AccApp09 Proc. AP/AM-07.
2. H. Sato, O. Takada, K. Iwase, T. Kamiyama and Y. Kiyanagi, J. Phys.: Conf. Ser. (accepted).
3. H. Sato, K. Morita, N. Ayukawa, T. Kamiyama and Y. Kiyanagi, JSNS2009 Proc. A-4 (in Japanese).
4. K. Iwase, K. Sakuma, T. Kamiyama and Y. Kiyanagi, Nucl. Instr. and Meth., **A605** (2009) 1.
5. S. Harjo, A. Moriai, S. Torii, H. Suzuki, K. Suzuya, Y. Morii, M. Arai, Y. Tomota, K. Akita and Y. Akiniwa, Mater. Sci. Forum **524-525** (2006) 199.
6. T. Ishigaki, A. Hoshikawa, M. Yonemura, T. Morishima, T. Kamiyama, R. Oishi, K. Aizawa, T. Sakuma, Y. Tomota, M. Arai, M. Hayashi, K. Ebata, Y. Takano, K. Komatsuzaki, H. Asano, Y. Takano and T. Kasao, Nucl. Instr. and Meth. **A600** (2009) 189.
7. http://j-parc.jp/MatLife/en/instrumentation/ns3.html
8. H. Sato, O. Takada, S. Satoh, T. Kamiyama and Y. Kiyanagi, Nucl. Instr. and Meth. A (submitted).
9. F. Maekawa, K. Oikawa, M. Harada, T. Kai, S. Meigo, Y. Kasugai, M. Ooi, K. Sakai, M. Teshigawara, S. Hasegawa, Y. Ikeda and N. Watanabe, Nucl. Instr. and Meth. **A600** (2009) 335.
10. K. Kaneko, T. Kamiyama, Y. Kiyanagi, T. Sakuma and S. Ikeda, J. Phys. Chem. Solids, **60** (1999) 1499.
11. T. Kamiyama, H. Noda, J. Ito, H. Iwasa, Y. Kiyanagi, S. Ikeda, J. Neutron Research, 13 (2005) 97; T. Kamiyama, J. Ito, H. Noda, H. Iwasa, Y. Kiyanagi, S. Ikeda, Nucl. Instrum. and Methods, **A 542** (2005) 258.
14. Pulsed neutron imaging using resonance transmission spectroscopy, H. Sato, T.Kamiyama and Y. Kiyanagi, Nucl. Instrum. and Methods, **A605(1-2)** (2009) 36-39.